16TH EUROPEAN CONFERENCE ON EARTHQUAKE ENGINEERING THESSALONIKI 18 - 21 JUNE 2018

THE PBEE PARADIGM IN CURRENT SEISMIC SAFETY ASSESSMENT CODES FOR EXISTING RC BUILDINGS: CONCEPTUAL AND STATISTICAL ASSESSMENT

Nuno PEREIRA[1], Xavier ROMÃO[2]

ABSTRACT

One of the main objectives of Performance-Based Earthquake Engineering (PBEE) is to allow for the direct analysis of a set of decision variables characterizing the response of a structure located in a specific site. Among these decision variables, loss metrics are particularly important due to their direct connection to the decisions related with retrofitting needs and post-earthquake reparability issues. Despite the recognized importance of these decision variables (DV) for stakeholder information and to develop adequate mitigation strategies, their explicit inclusion in current seismic safety assessment frameworks is still limited when assessing the performance of both new and older structures. Conversely, most of the assessments are based on engineering demand parameters (EDPs) such as interstorey drifts or component chord rotations, which are used as benchmarks to classify the damage states and the overall seismic performance of a building. This study analyses the compatibility between limit state component deformations and qualitative performance objectives defined in current seismic safety assessment standards such as the Eurocode 8 part 3 (EC8/3). A conceptual equivalence between the main principles adopted in the PEER-PBEE methodology and those included in the EC8/3 performance objectives is firstly established. After that, a statistical comparison between explicit (loss-based) and implicit (EDP-based) verifications of the performance objectives is performed based on 3 low-to-midrise RC buildings. The results show that logical loss values can be obtained for the implicit methods that are in line with the decision variables described for the corresponding performance objectives for the damage limitation and significant damage limit states.

Keywords: Reinforced Concrete, Eurocode 8-Part 3, Performance-based Earthquake Engineering, Performance objectives, Limit State conditions.

1. INTRODUCTION

Performance-based seismic assessment of buildings is a methodology that targets the evaluation of the seismic performance of a system when it is subjected to earthquake ground motions with different intensities. The main reason for the development of these methods stemmed from the observations made in the aftermath of the 1989 Loma Prieta and the 1994 Northridge earthquakes in California. After these events, stakeholders started to express some concerns regarding the performance of buildings, namely about the losses resulting from the damage in structural and non-structural components, despite ensuring life-safety conditions. Within this context, the main principles of performance-based earthquake engineering (PBEE) were developed, including explicit or implicit references to the human and economic consequences of the ground motion effects. One of the outcomes of this new philosophy was the definition of performance matrices as a complement to traditional safety assessment methods. These matrices, which were first introduced in American standards (SEAOC, 1995; ASCE, 2000), define the maximum damage that is allowed to occur in the structure as a consequence of a ground motion with a given intensity.

In Europe, one of the main developments introduced to create a unified approach to assess the seismic safety of existing reinforced concrete (RC) buildings was the publication of Part 3 of Eurocode 8 (EC8/3) (CEN, 2005). Similar to other standards available worldwide, EC8/3 establishes three classes of

[1]PhD student, CONSTRUCT-LESE, Faculty of Engineering, University of Porto, Portugal, nmsp@fe.up.pt
[2]Assistant Professor, CONSTRUCT-LESE, Faculty of Engineering, University of Porto, Portugal, xnr@fe.up.pt

performance objectives termed, in a decreasing order of expected damage, as Near Collapse (NC), Significant Damage (SD) and Damage Limitation (DL). These performance levels are qualitatively described in the standard in terms of admissible damage levels and deformations, and each class of performance objectives is connected to a specific level of seismic hazard (represented by a specific average return period). For NC, the performance objectives require the structure to still be able to sustain gravity loads after the ground motion, even though it may exhibit heavy damage and large permanent deformations. Conversely, the performance objectives associated with SD refer that non-structural components are expected to exhibit significant damage (although without out-of-the-plane collapse of infill walls). A structure compatible with the SD level is also expected to exhibit residual interstorey drifts with a moderate magnitude while still being able to sustain a moderate intensity aftershock without collapsing. EC8/3 also states that a structure exceeding the limit conditions associated with SD has a significant probability of being uneconomic to repair. Finally, the performance objectives associated with DL establish that no damage is expected in the structural elements while only minor damage, such as cracking of the infill walls, is expected for the non-structural components. Consequently, DL implies a post-earthquake state of the building with very low repair needs and assumes that no residual deformation has occurred in the building. The transitions between the performance or damage levels defined in EC8/3 are characterized by limit state conditions that establish limits above which the building is no longer compatible with a given performance class. Table 1 presents the referred damage states and the limits of the corresponding compliance criteria.

Table 1. Damage states and performance objectives defined in the current version of EC8/3.

Performance Objectives	**Structural Components**	**Non-structural Components**	**Permanent deformations**	**Reparable structure?**	**Compliance criteria**
Damage Limitation, DL	Light	Economical repair	Negligible	Yes	θ_{DL}
Significant Damage, SD	Significant	Damaged	Visible	Uneconomic	θ_{SD}
Near Collapse, NC	Heavy	Collapsed	Large	No	θ_{NC}, V_{NC}

As shown in Table 1, the compliance criteria for ductile elements defining the transition between the several damage limit states are defined in terms of local deformations (chord rotations, θ). Similar principles are also present in ASCE 41-13 (ASCE, 2013) and other codes. However, for the case of NC, the fragile failure of structural elements must also be analysed by assessing shear demand. These verifications are defined only for structural elements and connected to a specific level of seismic hazard compatible with the limit states, establishing the separation between the performance classes. If a single component exceeds a given limit state condition, the overall building is classified as non-compliant with that limit state. Hence, the considerations made regarding the state of non-structural components, the level of residual deformations, the capacity reserve against collapse or the level of repair losses are implicitly included in the limit state verifications. The Pacific Earthquake Engineering Research Centre (PEER) methodology was developed to answer the need for communicating seismic risk to stakeholders involving metrics that reflect seismic consequences and are different than the engineering terms usually adopted in earthquake engineering. This methodology allows for the quantification, in probabilistic terms, of different decision variables (DVs) such as monetary losses, repair time or number of fatalities. The basis of the PEER methodology lies in the probabilistic characterization of several performance metrics along with the multiple sources of uncertainty that are inherent to seismic assessment (e.g. the uncertainty about the hazard, the ground motions representing a seismic scenario, the modelling and knowledge-based uncertainties of the building components and properties). The PEER methodology can be summarized into the framing equation representing the rate of a certain DV exceeding a value *dv* (Cornell and Krawinkler, 2000):

$$\lambda(\mathrm{DV}>\mathrm{dv}) = \int_{\mathrm{IM}}\int_{\mathrm{EDP}}\int_{\mathrm{DM}} G(\mathrm{DV}|\mathrm{DM})\cdot\left|dG(\mathrm{DM}|\mathrm{EDP})\right|\cdot\left|dG(\mathrm{EDP}|\mathrm{IM})\right|\cdot\left|d\lambda(\mathrm{IM})\right| \quad (1)$$

where DM represents a damage measure, generally discretised into several damage states, EDP represents a measure of the structural response that can be correlated with DM, IM is a ground motion

intensity measure and G(·) is the complementary cumulative distribution function. The numerical integration of Eq. (1) can be used to estimate the annual losses. A discrete solution of Eq. (1) requires the quantification of the expected loss value, $E(L|IM_i)$, for each ground motion intensity IM_i, and can be estimated from the proposal of Ramirez and Miranda (2009), based on previous work by Aslani (2005):

$$E\left(L \mid IM_i\right) = E\left(L \mid \overline{C} \cap R, IM_i\right) \cdot p\left(\overline{C} \cap R \mid IM_i\right) + E\left(L \mid \overline{C} \cap D, IM_i\right) \cdot p\left(\overline{C} \cap D \mid IM_i\right) + \\ + E\left(L \mid C, IM_i\right) \cdot p\left(C \mid IM_i\right) \tag{2}$$

where $E\left(L \mid \overline{C} \cap R, IM_i\right)$, $E\left(L \mid \overline{C} \cap D, IM_i\right)$ and $E\left(L \mid C, IM_i\right)$ are the expected value of the losses for IM_i given that the structure is still reparable (without collapsing), the expected value of the losses for IM_i given that the structure is not reparable (without collapsing) and the expected value of the losses for IM_i given that the structure will collapse, respectively. The probabilities of having a reparable and an irreparable building without collapsing can be calculated by factorizing the corresponding probability of demolition $p\left(D \mid \overline{C}, IM_i\right)$ by the probability of collapse, $p\left(C \mid IM_i\right)$. Finally, the expected value of the losses for a given ground motion intensity IM_i can be quantified considering a relative quantity, the loss ratio, defined by the ratio between the obtained losses and the cost of replacing the structure. This implies that the loss ratio is 1.0 when the structure is considered irreparable or when structural collapse is observed, and Eq. (2) becomes:

$$E\left(L \mid IM_i\right) = E\left(L \mid \overline{C} \cap R, IM_i\right) \cdot \left[1 - p\left(D \mid \overline{C}, IM_i\right)\right] \cdot \left[1 - p\left(C \mid IM_i\right)\right] + \\ + p\left(D \mid \overline{C}, IM_i\right) \cdot \left[1 - p\left(C \mid IM_i\right)\right] + p\left(C \mid IM_i\right) \tag{3}$$

A closer analysis of EC8/3 performance objectives (Table 1) shows that most variables currently used to estimate losses, as those included in Eq. (3), have to be controlled for each limit state. Hence, in principle, thresholds associated with maximum expected losses can be defined in the same way that local demand limits are employed in current standards, since they explicitly represent the conditions qualitative defined by the performance objectives. Nevertheless, to the authors' knowledge, a solid conceptual and statistical evaluation of the equivalence between the implicit and the explicit verification of the performance objectives described in EC8/3 has not yet been conducted. As such, the proposed study aims to assess the extent of this equivalence, analysing the conceptual similarities between current code methods and the PEER-PBEE, and evaluating the statistical equivalence between the results obtained with both formulations for the specific case of existing mid-rise RC moment resisting frame (RC-MRF) buildings.

2. METHODOLOGY

2.1 General approach

Three RC-MRF buildings were considered in the present study. These buildings consist of structures regular in plan and in elevation designed without capacity design rules. The plan view of the building and of the structure, the sectional details (common to all buildings) and the elevation view of the buildings with 3 (REG3), 4 (REG4) and 5 (REG5) storeys can be found in Fig. 1. The three buildings analysed have masonry infill walls with a thickness of 0.15m and openings in all spans apart from that of the staircase façade where glass panels were considered. The stairs are composed of slabs simply supported by beams, unloading on the beams of the floor levels and on mid-height beams located at each storey. Regarding the material properties, a mean concrete compressive strength and a mean reinforcing steel yielding strength of 25 MPa and 500 MPa were adopted, respectively. The masonry compressive strength was assumed to be 3.10 MPa. A permanent load equal to 4 kN/m^2 was uniformly distributed across all slabs, in addition to the self-weight of the horizontal elements. A uniform live load of 3 kN/m^2 was also assigned to all slabs, with the exception of the roof where the live load was reduced to 1 kN/m^2.

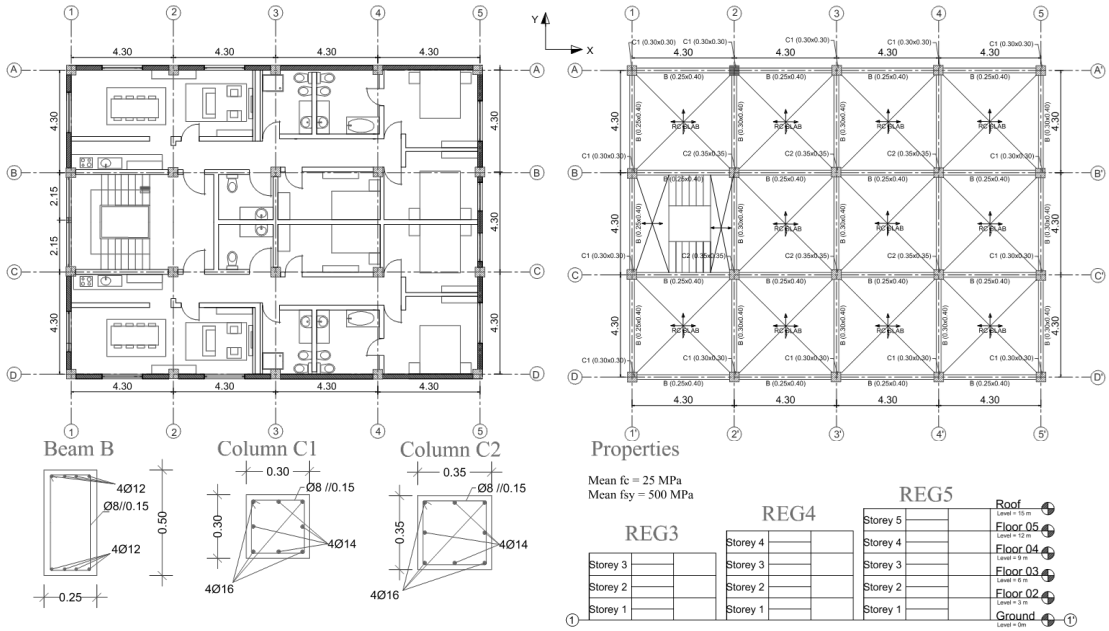

Figure 1. Properties of the three selected buildings.

The stair slabs were only considered through their equivalent permanent and live loading distributed on the supporting beams. The weight of the masonry infills was defined as a uniform load (7 kN/m) applied to the supporting beams of the peripheral frames. The fundamental periods of the analysed buildings are 0.31sec; 0.25 sec (REG3), 0.41 sec; 0.31 sec (REG4) and 0.52 sec; 0.39 sec (REG5) for the fully infilled building and 0.73sec; 0.72 sec (REG3), 0.96 sec; 0.93 sec (REG4) and 1.18 sec; 1.15sec (REG5) when the masonry infills were not considered for the initial stiffness (i.e. bare frame conditions).

A 3D nonlinear model of each building was created using the OpenSees platform (McKenna *et al.*, 2000). Beam-column elements were modelled using nonlinear moment-rotation springs at the ends of all elements. The axial load and the moment interaction between the two orthogonal directions of the transversal sections of the columns was not considered, with independent flexural springs calibrated using the axial loads from the gravity load analysis being assigned to each direction. The moment rotation behaviour of each spring was defined using a trilinear curve defined by the yielding moment approximation (M_y) and yielding rotation (θ_y) proposed by Panagiotakos and Fardis (2001), the capping rotation θ_c (corresponding to a maximum moment of $1.14 \cdot My$) and the post-capping rotation (θ_{pc}) following the proposal of Haselton *et al.* (2016). Damping and stiffness of the structural elements were adjusted based on the recommendations of Zareian and Medina (2010). Beam-column joints were assumed to be rigid. This assumption was made since it corresponds to the most commonly considered approach made by analysts applying current seismic safety assessment methods. Finally, the infills located at peripheral frames (apart from the staircase façade) were modelled using a single strut model, following the recommendations of Dolšek and Fajfar (2008).

The three benchmark buildings were considered to be located in Lisbon, Portugal, with foundations in a soil of type B (CEN, 2010). Incremental dynamic analysis (Vamvatsikos and Cornell, 2002) was used to evaluate the response of the buildings for increasing values of the ground motion intensity level (IML). Each building was analysed up to collapse, this being defined by numerical instability of the nonlinear model for a given IML of each ground motion record. The IML corresponding to the selected performance criteria was determined using the hunt and fill algorithm (Vamvatsikos and Cornell, 2004). In total, 160 pairs of ground motion records were used in each IDA analysis. Due to the specificities of the Portuguese seismic hazard, 40 (40) pairs of records were selected using SelEQ (Macedo and Castro, 2017) matching the average of the geometric mean of the two as-recorded components to the Type I (II) response spectrum as presented in the national annex to the Eurocode 8-Part 1 (CEN, 2010). Individual control of the goodness of fit of each pair of records was also imposed.

The selected pairs of records were considered with angles of 0º and 90º, following the recommendations of current guidelines (i.e. FEMA-P58, 2012). The intensity measure adopted in the IDA consisted in the geometric mean of the 5% damped spectral acceleration, $AvgS_a$, considering the periods T_{1xinf} (T_{1yinf})

computed using the infilled frame structure (see x and y directions in Fig. 1), $T_{1x,bare}$ ($T_{1y,bare}$) and $2T_{1x,bare}$ ($2T_{1y,bare}$) computed using only the bare frame structure. In that way, a period corresponding to different behaviour ranges of the structure is included in the IM definition. Details about the more generic use of $AvgS_a$ can be found e.g. in Kohrangi *et al.* (2016). The results of the IDA were post-processed considering as decision variables the maximum (over all structural elements) chord rotation demand-to-capacity ratio attained for each ground motion case and for each IML (implicit approach) and the expected value of the losses due to the damage induced by each ground motion case and each IML (explicit approach). The adoption of the different criteria aimed at establishing an objective approach that could be used to compare the results of different limit state conditions defined using implicit (based on current standard-based methods) or explicit (based on the loss-based approach) verifications of the performance objectives described in Table 1. After the processing of the EDP-based and loss-based criteria, IDA curves for all the 160 ground motion pairs were computed and the distribution of the $AvgS_a$ levels leading to the performance criterion was computed. Finally, a statistical comparison between the $AvgS_a$ distributions obtained using the implicit and the explicit performance-based criteria was performed.

2.2 Implicit verifications of the performance objectives

The implicit approach adopted for the post-processing of the IDA results involved the analysis of local demands which are considered to be a proxy for the building performance, as assumed in current seismic safety assessment standards. Scalar damage variables were analysed with a generic format given by:

$$Y_{LS} = \frac{\theta_{\mathrm{D}}}{\theta_{\mathrm{R},LS}} = \max\left(\frac{\theta_{\mathrm{D,x}}}{\theta_{\mathrm{R},LS,\mathrm{x}}}; \frac{\theta_{\mathrm{D,y}}}{\theta_{\mathrm{R},LS,\mathrm{y}}}\right), \tag{4}$$

where θ_D represents the maximum demand in terms of chord rotations, $\theta_{R,LS}$ is defined as a damage limit state threshold and x and y represent the main sectional directions of each element. Scalar damage variables were calculated for every component of the building. Several proposals can be found in the literature to establish $\theta_{R,LS}$ (e.g. CEN, 2005; Haselton *et al.* 2016; Grammatikou *et al.* 2017). As defined in Table 1, three damage limit states (damage limitation, DL, significant damage, SD and near collapse, NC) are available in EC8/3 that are compatible with different performance objectives (see Table 1). Accordingly, these damage limit states were adopted in the implicit approach. The θ_{DL} limit was computed according to the proposal of EC8/3. The remaining limits were computed using the empirical models derived by Haselton *et al.* (2016), according to which θ_{SD} is computed by adding $\theta_{cap,pl}$ (see Haselton *et al.* (2016)) to θ_{DL}; θ_{NC} was defined as 4/3 of θ_{DL} following a similar principle to that of EC8/3. In addition to these cases, the ultimate limit θ_C was defined as the sum of θ_{DL} and θ_{pc} (see Haselton *et al.* (2016). Figure 2 summarizes the Y_{LS} conditions adopted and presents vertical lines representing the demand-to-capacity ratios that correspond to the condition Y_{LS}=1 for DL, SD, NC and C. For each ground motion record and IML, the maximum of Y_{DL}, Y_{SD}, Y_{NC} and Y_C was computed, yielding 160 IDA curves used to determine the probability distribution of the AvgSa leading to Y_{LS}=1.

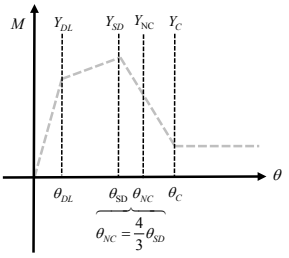

Figure 2. Capacity of each flexural spring and corresponding limit states.

2.3 Explicit verifications of the performance objectives

For the case of the explicit verification of performance objectives, a similar rationale was adopted to define a new Y_{LS} condition using a direct loss-based approach. Accordingly, Y_{LS} was defined as the ratio

between the expected loss value and a limit value representing the corresponding limit state capacity:

$$Y_{LS} = \frac{L \mid m}{L_{m,LS}} \tag{5}$$

where $L|m$ represents the expected value of the losses induced to the structure due to the occurrence of a given ground motion m and $L_{m,LS}$ represents a threshold for the expected value of the losses. Both quantities can be normalized by the replacement cost, leading to loss values between 0 and 1.0.
For each ground motion, the quantification of $L|m$ was defined using the principles outlined in Eq. (3). The condition that explicitly evaluates the performance objectives described before is defined as:

$$L \mid m = \begin{cases} E\left[L \mid m\right] \cdot \left[1 - \Phi\left(\frac{\ln\left[RIDR\right] - \ln\left[0.015\right]}{0.3}\right)\right] + \Phi\left(\frac{\ln\left[RIDR\right] - \ln\left[0.015\right]}{0.3}\right) & \text{if } \overline{C} \\ 1.0 & \text{if } C \end{cases} \tag{6}$$

which includes the expected value of the repair costs $E[L|m]$, the loss component related to the probability of demolition given the permanent deformations (RIDR) exhibited by the building when subjected to ground motion m and, indirectly, the probability of collapse by assigning a value of 1.0 to $L|m$ if the collapse criterion defined by the numerical instability condition is attained. In the explicit approach, the probability of demolition was represented according to Ramirez and Miranda (2012). Hence, the probability of demolition was calculated using the value of the maximum residual IDR (RIDR) considering that the referred probability follows a lognormal distribution with a mean RIDR of 0.015 and a dispersion of 0.30. The approach adopted to quantify the repair losses was based on the storey-based approach proposed by Zareian and Krawinkler (2006) and Ramirez and Miranda (2009). To derive these functions, three classes of building components were selected: interstorey drift (ISR) -sensitive structural elements (S|IDR), IDR-sensitive non-structural components (NS|IDR) and peak floor acceleration (PFA) -sensitive non-structural components (NS|PFA). The development of engineering demand parameters to loss (EDP-to-Loss) functions for these three classes was done following the strategy adopted by Ramirez *et al.* (2012). Fragility functions for these classes of components were collected from HAZUS-MH MR4 (FEMA, 2003) for low-code C3L (low-rise concrete frame with unreinforced masonry infill walls with 1-3 storeys) and C3M (mid-rise concrete frame with unreinforced masonry infill walls with 4-7 storeys) buildings. These fragility functions were crossed with the median consequence models proposed in HAZUS-MH MR4 (FEMA, 2003) for multi-family dwellings (RES3). By assuming the expected value of the consequences and simulating the fragility functions for different values of IDR and PFA. A normalized $E[L|EDP]$ curve (between 0 and 1 where 1 represents the total loss of the class of components) were created for each class of components. Following the indications in Martins *et al.* (2015), a weight of 85% was assigned to the IDR-sensitive component losses (L|IDR) including 20% of losses related with structural components (S|IDR) and 65% with the non-structural counterpart (NS|IDR). Finally, following the same component aggregation for a residential building in Portugal, 15% of the losses were assigned to the repair needs of PFA sensitive components (L|PFA). The resulting EDP-to-Loss functions are shown in Fig.3.
As mentioned, the principles adopted by Ramirez *et al.* (2012) were followed, thus leading to EDP-to-Loss curves not at the building level but at the storey-level. Therefore, $E[L|m]$ was calculated using:

$$E\left[L \mid m\right] = \frac{1}{n_{storeys}} \cdot \sum_{i=1}^{nstoreys} \frac{1}{2} \cdot \left(L \mid IDR_{x,i} + L \mid IDR_{y,i}\right) + \frac{1}{n_{floors}} \cdot \sum_{j=1}^{nfloors} \max\left(L \mid \mathrm{PFA}_{x,j}, L \mid \mathrm{PFA}_{y,j}\right) \tag{7}$$

which implies the assumption that all storeys have the same configuration (and therefore value), the averaging of the losses between the two directions of the building, thus assuming a similar distribution of drift- sensitive non-structural elements along the x and y as well as an average damage level induced to structural elements. In Eq.(7), n_{floors} refers to the number of ceilings (see Fig. 1) that have acoustic panels and lighting equipment. In total, 160 vulnerability curves were generated for all the pairs of the

considered ground motion records and, based on these IDA curves, $AvgS_a$ distributions corresponding to normalized loss thresholds from 0.01 to 1.00 in steps of 0.01 were computed.

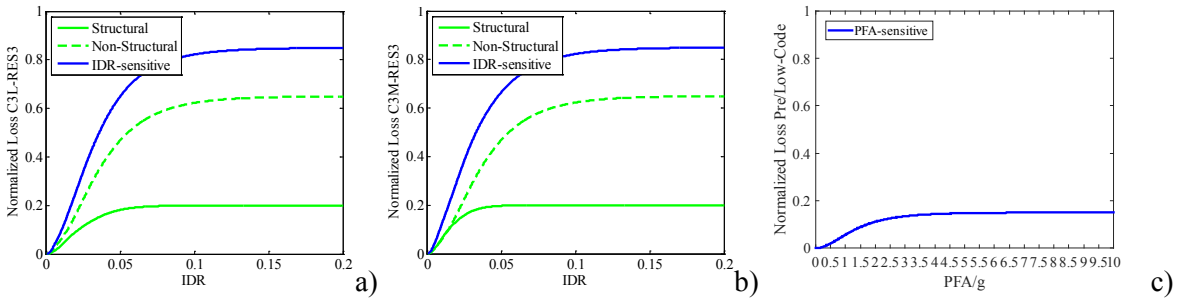

Figure 3. EDP-to-Loss curves adopted for the evaluation of the expected loss value due to the maximum IDR and PFA values resulting from a given ground motion.

2.4 Statistical analysis

The $AvgS_a$ distributions were analysed using median and standard deviation (SD) values. The comparison between the distributions of the $AvgS_a$ values leading to the conditions Y_{DL}=1, Y_{SD}=1, Y_{NC}=1, Y_C=1 and those associated to the 100 normalized loss thresholds was made considering three different strategies. The comparison of the medians of the distributions was done using the Kruskal-Wallis test (KW; Kruskal and Wallis, 1952) to evaluate if the EDP-based and the loss-based $AvgS_a$ distributions could be assumed has samples of the same distribution. Similarly, the Brown–Forsythe test (BF, Brown and Forsythe, 1974) was adopted to evaluate the equality of the variances of the different samples of $AvgS_a$. A critical value of 0.05 for the p-value was considered in these tests. Additionally, the two-sample Kolmogorov-Smirnov (KS, Marsaglia *et al.*, 2003) distance was also adopted to measure the overall differences between the EDP-based and the loss-based $AvgS_a$ distributions.

3. RESULTS

Figure 4 presents the IDA curves obtained for the maximum values of Y_{DL}, Y_{SD}, Y_{NC} and Y_C for structures REG3, REG4 and REG5. The limit lines corresponding to Y_{DL}=1, Y_{SD}=1, Y_{NC}=1, Y_C=1 are also presented. The median (SD) $AvgS_a$ leading to the condition Y_{DL}=1 was found to be 0.176g (0.046g), 0.149g (0.037g) and 0.117g (0.030g) for the REG3, REG4 and REG5, respectively. For the Y_{SD}=1 condition, the median (SD) values obtained for building REG3 was 0.666g (0.151g), while lower values were observed for REG4 (0.477g (0.113g)) and for REG5 (0.392g (0.080g)). The NC limit state condition Y_{NC}=1 was observed for median (SD) $AvgS_a$ values of 0.798g (0.198g), 0.602g (0.148g) and 0.457g (0.111g), with similar values being also observed for the Y_C=1 (0.900g (0.243g), 0.694g (0.174g) and 0.536g (0.126g) for the REG3, REG4 and REG5, respectively).

Figure 5 shows the evolution of the distributions of the $AvgS_a$ values obtained for incremental levels of the admissible normalized loss ($L_{m,LS}$) for buildings REG3 to REG5. An approximate trilinear curve was obtained for the median $L_{m,LS}$ - $AvgS_a$ curve in all cases. The first branch of the curve develops until a $L_{m,LS}$ value of 0.20. Similarly, in all cases, a subsequent linear branch with a smaller slope is observed until a value of $L_{m,LS}$ around 0.50 is reached. Finally, the third branch of the curve represents a region with a very small increment of the $AvgS_a$ and a large increase of the losses.

Figure 6 shows the comparison of the distributions of the $AvgS_a$ values leading to the condition Y_{LS}=1 with the 100 distributions of the same IML for different $L_{m,LS}$ thresholds. The results presented refer to the evolution of the p-values of the Kruskal-Wallis and of the Brown.-Forsythe tests and their corresponding comparison with the assumed critical value (0.05). As seen in Figs. 6a-6c, the KW test applied to the distribution associated with Y_{DL}=1 yields maximum p-values of 0.08, 0.69 and 0.91 for values of the normalized loss $L_{m,DL}$ of 0.03, 0.04 and 0.04, for buildings REG3, REG4 and REG5, respectively. Similar results are observed for the BF test. The p-value range above the critical limit is wider (around 0.03-0.09 instead of 0.03-0.04). The maximum p-values observed (0.81, 0.86 and 0.83) correspond to $L_{m,DL}$ limits of 0.03, 0.05 and 0.05 for REG3, REG4 and REG5, respectively. Figures 6d-6f present the evolution of the p-values of the KW and BF tests for increasing levels of the normalized loss considering as a reference the condition Y_{SD}=1. In this case, $L_{m,SD}$ values of 0.20-0.31 are found to

be compatible with the higher p-values of the KW test (0.81; 0.66; 0.63). Similar values of $L_{m,SD}$ (0.27; 0.37; 0.42) are also observed when analysing the maximum p-values obtained when applying the BF test. The range of the $L_{m,SD}$ values above the critical p-value (0.25-0.47) is wider than the one obtained for the DL limit state.

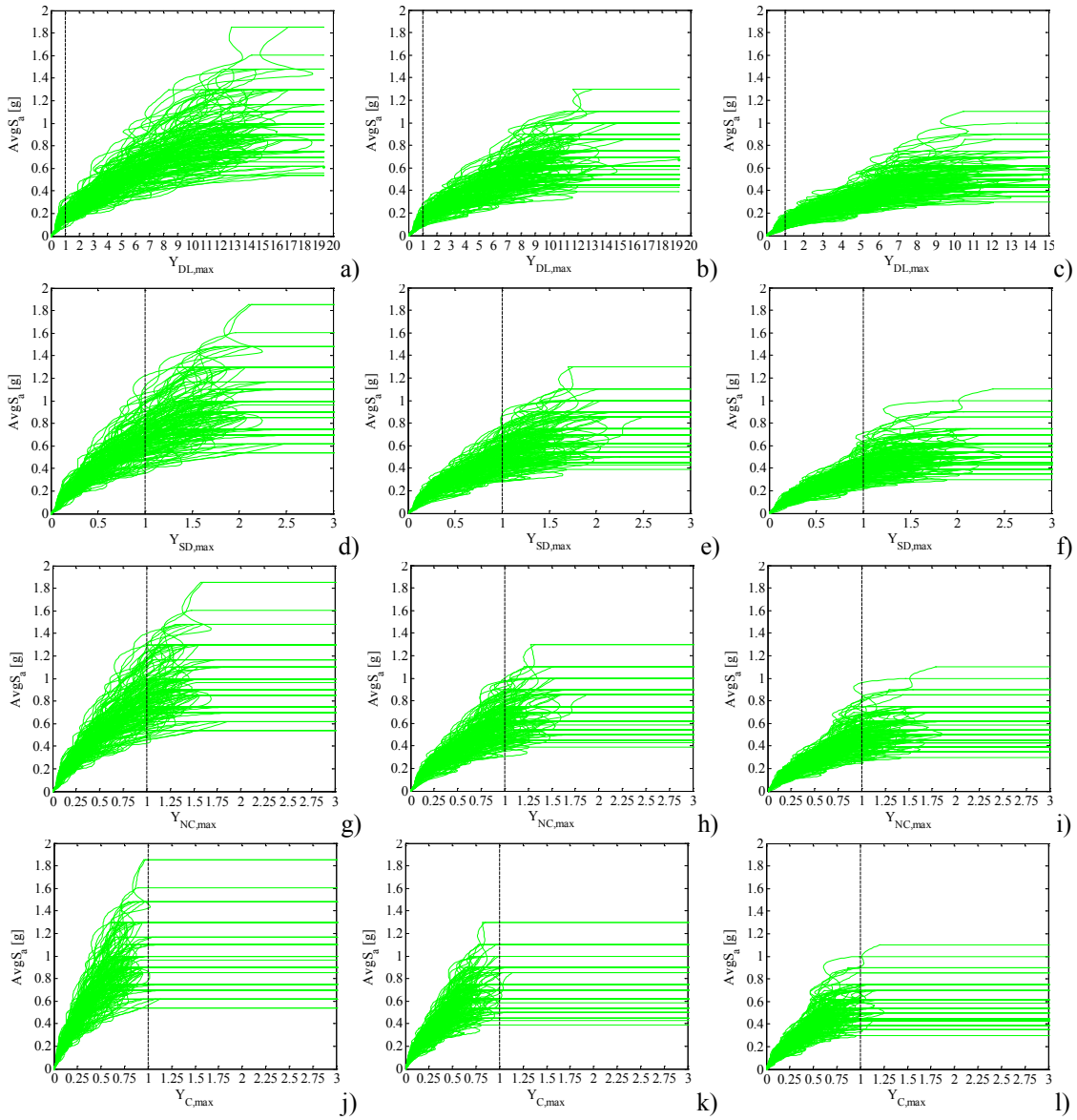

Figure 4. IDA curves for the maximum values of the Y_{DL} (a, b, c), Y_{SD} (d, e, f), Y_{NC} (g, h, i) and Y_C (j, k, l) for building REG3 (a, d, g, j), REG4 (b, e, h, k) and REG5 (c, f, i, l).

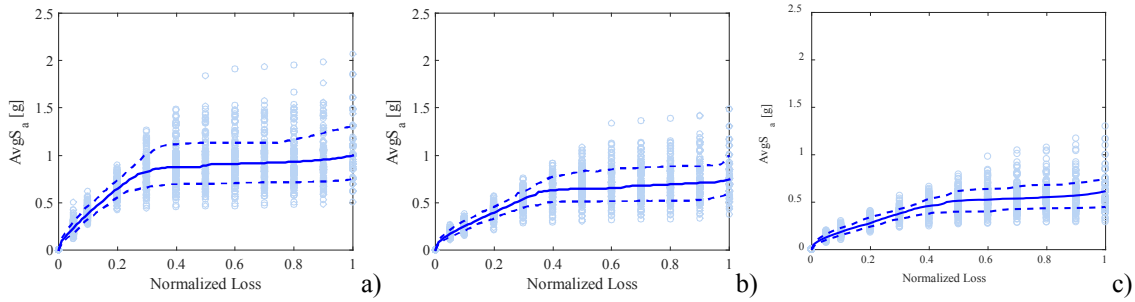

Figure 5. Evolution of the $AvgS_a$ values associated with different normalized loss limits for buildings REG3 (a), REG4 (b) and REG5 (c).

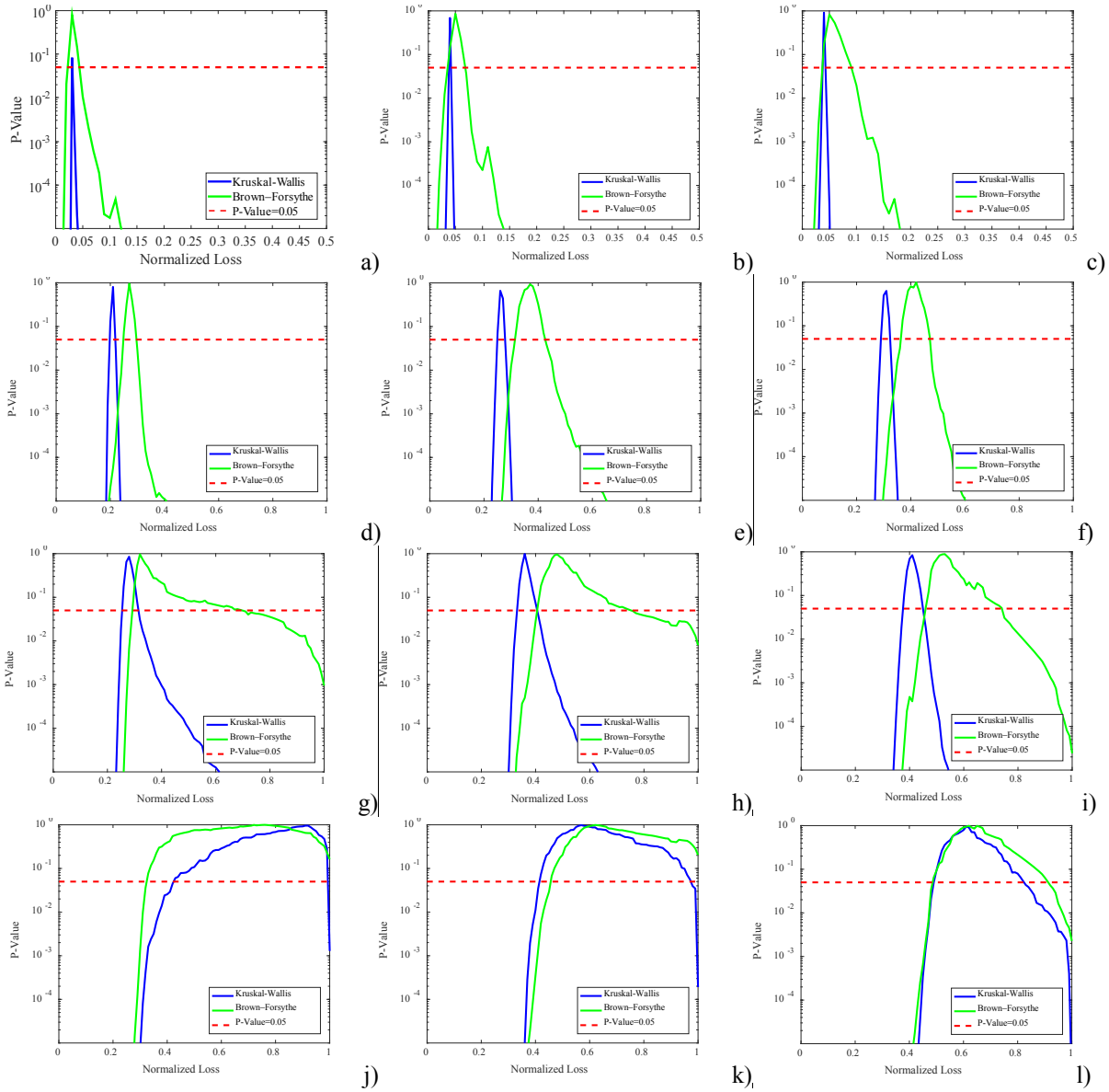

Figure 6. Results of the KW and BF tests applied when using as a reference the distribution of AvgSa values compatible with Y_{DL} (a, b, c), Y_{SD} (d, e, f), Y_{NC} (g, h, i) and Y_C (j, k, l) for building REG3 (a, d, g, j), REG4 (b, e, h, k) and REG5 (c, f, i, l).

The results for the NC limit state condition Y_{NC}=1 are shown in Figs. 6g-6i. The $L_{m,NC}$ limit values tah are seen to have a higher compatibility with the Y_{NC}=1 condition are 0.28, 0.36 and 0.41 according to the results of the KW test (p-values of 0.85, 0.99, and 0.84), and 0.32, 0.48 and 0.53 according to the BF test (p-values of 0.96, 0.96 and 0.89), for REG3, REG4 and REG5, respectively. Nevertheless, for the BF test, the range of values compatible with the critical p-value are wider and range from 0.30, 0.41 and 0.46 to 0.69, 0.75 and 0.74, respectively. For the KW test, the range of values compatible with the critical p-value is limited to 0.46-0.75. Different results are obtained when the condition Y_C=1 is evaluated (Figs. 6j-6l).). In this case, it can be seen that p-values above 0.95 are obtained for all cases and for both tests. The $L_{m,C}$ values that are statistically compatible with the condition Y_C=1 are 0.92, 0.57 and 0.61 according to the maximum p-value obtained using the KW test, and 0.76, 0.62 and 0.62 when the BF test is used (for REG3, REG4 and REG5, respectively). The range of $L_{m,C}$ values obtained using both tests that verify the selected critical p-value are within the range 0.49-0.91.

Figure 7 complements the above information by showing the maximum absolute difference between the ordinates of the cumulative distribution functions (CDFs) of the $AvgS_a$ values corresponding to the Y_{LS} conditions and those obtained assuming different $L_{m,LS}$ limits (KSstat), using the KS distance.

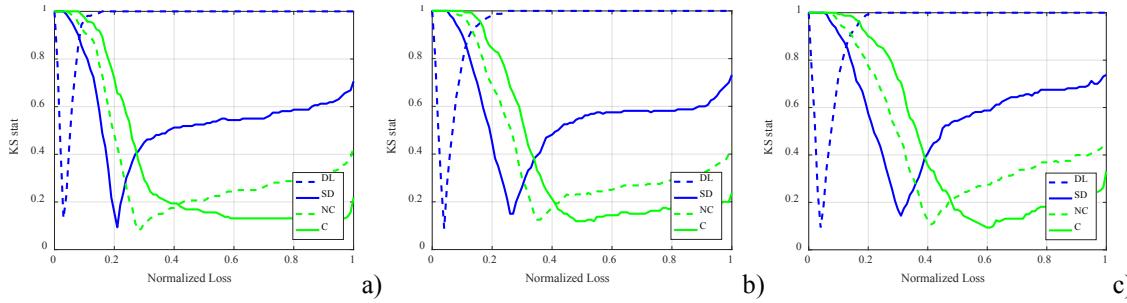

Figure 7. Evolution of the distance obtained using the two-sample Kolmogorov-Smirnov distance between the distribution of $AvgS_a$ values referring to the Y_{LS} = 1 conditions that are obtained for different levels of the admissible normalized loss for buildings REG3 (a), REG4 (b) and REG5 (c).

As seen in Fig. 7, for Y_{DL} = 1, the minimum value of KSstat occurs for a $L_{m,DL}$ value of 0.03, 0.04 and 0.04, for REG3, REG4 and REG5, respectively. For the Y_{SD} = 1, the $L_{m,SD}$ values that minimize KSstat are now 0.21, 0.26, 0.31, while for Y_{NC} = 1 they are 0.28, 0.35 and 0.41. For Y_C = 1, it can be seen that the minimum distance between the CDFs does not change considerably after reaching $L_{m,C}$ = 0.40, thus corroborating the main results presented in Figs. 6j-6l. Figure 8 shows the disaggregation of the losses corresponding to the mean $AvgS_a$ leading to the condition Y_{DL}=1. It can be seen that losses associated with the PFA-sensitive non-structural components (NST-PFA) are responsible for the largest contribution, whose global value is in the order of 3-4%. Structural losses (ST) and losses in drift-sensitive components (NST-IDR) have a very low contribution. The difference between the average loss value and the sum of the losses attributed to IDR and PFA-sensitive components (Total - ST&NST, used as a proxy for collapse and residual deformations) has an insignificant or null value in all cases (in both cases represented as <1%). Figure 9 shows results similar to those of Fig. 8 for the condition Y_{SD}=1. In this case, 20-30% of the total average loss can be associated with structural components, but the major component (40-45%) is due to the repair needs of IDR-sensitive non-structural components. In total, the losses of non-structural components account for 60-70% of the total average loss. The component Total-ST&NST has a low contribution, reflecting the lower influence of collapse in the total losses.

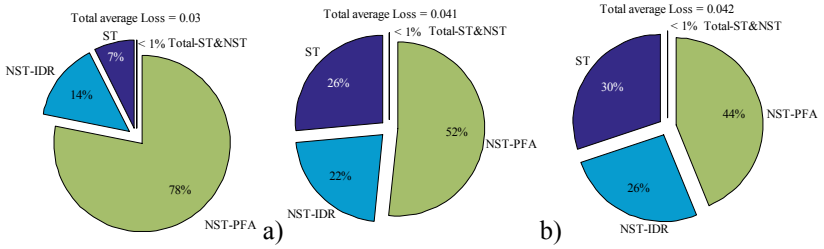

Figure 8. Disaggregation of the losses corresponding to the mean $AvgS_a$ leading to the condition Y_{DL}=1 in buildings REG3 (a), REG4 (b) and REG5 (c).

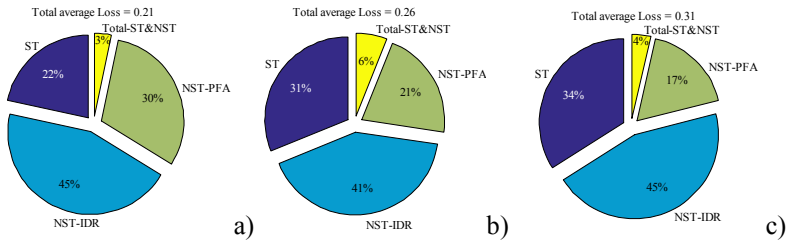

Figure 9. Disaggregation of the losses corresponding to the mean $AvgS_a$ leading to the attainment of the condition Y_{SD}=1 in buildings REG3 (a), REG4 (b) and REG5 (c).

4. DISCUSSION

The statistical analyses and comparisons performed in the present study indicate that, for the selected structures, i.e. mid-rise RC infilled frames, regular in plan and in elevation, and designed without capacity-design, there is a compatibility between the philosophy adopted in present seismic safety assessment standards and the full probabilistic PBEE principles. As referred by EC8/3, the DL limit

state considers a low level of damage in structural elements and damage to non-structural components that is economical to repair. Results show that the Y_{DL} = 1 condition is statistically equivalent to a normalized loss $L_{m,DL}$ close to 5% of the replacement cost. Previous studies (Romão *et al.*, 2014) using 2D frames reached similar conclusions regarding the amount of losses (6% of the total loss was computed for Y_{DL} = 1). Due to the properties of the Y_{DL} = 1 condition, limited losses are induced to structural elements, which may only present minor cracking due to the pre-yielding state of most components. Therefore, most of the losses are attributed to the damage in non-structural elements, particularly since plastic deformations are not expected for Y_{DL} = 1. The considerable level of damage found for NST-PFA components implies that some repairs may be required, although their expected extent is still expected to be compatible with the DL performance objectives.

For the SD limit state, the computed $L_{m,SD}$ values were seen to be within the range 0.20-0.40. Interestingly, these values are in line with the recommendations made by FEMA P-58 (FEMA 2012) and the results provided by Ramirez and Miranda (2012). FEMA (2012) suggests that 40% can be seen as a reasonable limit for many buildings. Hence, the results obtained for the three buildings imply that the Y_{SD} = 1 condition can be seen as equivalent to the performance objectives defined for SD in Table 1, since the governing condition is related with the fact that a building in such state may be uneconomic to repair. Romão *et al.* (2014) found a loss value of 0.17 compatible with the Y_{SD} = 1 condition. Nevertheless, these authors did not include the losses in the PFA-sensitive components, which can contribute to the lower values that were found. As shown in Fig. 9, the amount of losses attributed to the structural elements is in the range 20-35% of the overall total, thus approximately 1/4 of the total replacement value of these elements. Similar relative values (25%) were found for the losses induced to NST-IDR. The PFA-sensitive elements showed loss values of about 1/3 of their total replacement. These values are compatible with the SD performance objectives, where non-structural elements are expected to be significantly damaged.

5. CONCLUSIONS

Current standard-based methods for seismic performance assessment use compliance criteria that are expected to aggregate the main probabilistic principles inherent to performance objectives. However, analysing the equivalence of standard-based methods and probabilistic approaches in a more global way instead of on a case-by-case situation is not straightforward. The loss assessment procedure considered in the current paper addresses this issue by involving a simplified loss assessment approach derived from storey-based loss assessment methods. The use of this simplified method supports the development of a more generalized analysis of the referred equivalences, since it considers general loss functions that avoid the need for an extensive inventory of building components.

The conceptual comparison presented herein shows that performance objectives currently defined in EC8/3 include a qualitative description of all the main principles also adopted in probabilistic PBEE methods. The performance objectives are clearly defined in terms of decision variables that are also used in modern PBEE methods (repair costs) and include explicit settings which resemble the weighting scheme associated with demolition and collapse probabilities. This study as shown that for the three analysed regular RC-MRF buildings with infill walls, the compliance criteria based on chord rotations have a statistical equivalence with expected loss values (defined based on conditions of general methods such as the HAZUS approach) found in the literature as representative of similar performance levels.

Furthermore, despite potential limitations that may be associated with the proposed storey-based approach, it nevertheless provides a more consistent correlation between the building-specific assessments proposed by current standards and the more generalized seismic risk assessment strategies.

6. REFERENCES

SEAOC Vision 2000 Committee (1995): Performance-based seismic engineering. SEAOC, Sacramento, CA.

American Society of Civil Engineers (2000): Pre-standard and commentary for the seismic rehabilitation of buildings, Report No. FEMA-356, Washington, D.C.

CEN (2005): ENV 1998-3. Eurocode 8: Design of structures for earthquake resistance - Part 3: Assessment and retrofitting of buildings. European Committee for Standardization, Brussels, Belgium.

ASCE (2013). Seismic Evaluation and Retrofit of Existing Buildings (ASCE/SEI 41-13). American Society of Civil Engineers, Reston, Virginia, USA.

Cornell CA, Krawinkler H (2000). Progress and challenges in seismic performance assessment, PEER Centre News 3(2):1-3.

Ramirez CM, Miranda E (2009): Building-specific loss estimation methods & tools for simplified performance-based earthquake engineering. Report No. 171. John A. Blume Earthquake Engineering Research Centre. Stanford University. Stanford, California.

Aslani H (2005): Probabilistic earthquake loss estimation and loss disaggregation in buildings. PhD Dissertation. Stanford University.

McKenna F, Fenves GL, Scott MH, Jeremić, B (2000). Open system for earthquake engineering simulation ⟨http://opensees.berkeley.edu⟩

Panagiotakos TB, Fardis MN (2001). A displacement-based seismic design procedure for RC buildings and comparison with EC8. *Earthquake Engineering & Structural Dynamics*, 30: 1439–1462.

Haselton CB, Liel AB, Taylor-Lange SC, Deierlein GG. (2016). Calibration of model to simulate response of reinforced concrete beam-columns to collapse. *ACI Structural journal.* 113(6): 1141-1152.

Zareian F, Medina RA (2010): A practical method for proper modeling of structural damping in inelastic plane structural systems. *Computers & structures*, 88(1): 45-53.

Dolšek M, Fajfar, P (2008). The effect of masonry infills on the seismic response of a four-storey reinforced concrete frame – a deterministic assessment, *Engineering Structures*, 30, 1991-2001.

CEN (2004). Eurocode 8 : Design of structures for earthquake resistance - Part 1: General rules, seismic actions and rules for buildings (EN 1998-1:2004). European Standard NP EN. CEN, Brussels.

Vamvatsikos D, Cornell CA (2002). Incremental dynamic analysis. *Earthquake Engineering & Structural Dynamics*, 31(3): 491-514.

Vamvatsikos D., Cornell C.A. (2004). Applied Incremental Dynamic Analysis. *Earthquake Spectra*, 20(2): 523-553. (http://users.ntua.gr/divamva/software.html).

Macedo L, Castro JM (2017). SelEQ: An advanced ground motion record selection and scaling framework. *Advances in Engineering Software*. 114: 32–47.

FEMA (2012) Next-Generation Methodology for Seismic Performance Assessment of Buildings, prepared by the Applied Technology Council for the Federal Emergency Management Agency, Report No. FEMA P-58, Washington, D.C.

Kohrangi M., Bazzurro P, Vamvatsikos D (2016). Vector and scalar IMs in structural response estimation: Part II - Building Demand Assessment. Earthquake Spectra. *Earthquake Spectra*, 32(3): 1525-1543.

Grammatikou S, Biskinis D, Fardis MN (2017) Flexural rotation capacity models fitted to test results using different statistical approaches. *Structural Concrete*, 1–17.

Zareian F, Krawinkler H (2006): Simplified performance-based earthquake engineering. Report No. 169. John A. Blume Earthquake Engineering Research Centre. Stanford University. Stanford, California.

Ramirez CM, Gupta A, Myers A (2012). Detailed seismic loss estimation for a tall building in Japan. 15th World Conference on Earthquake Engineering, Lisbon, Portugal.

FEMA (2003). HAZUS-MH MR4, Technical manual, Department of Homeland Security—Federal Emergency Management Agency.

Martins L, Silva V, Marques M, Crowley H, Delgado R (2015): Development and assessment of damage-to-loss models for moment-frame reinforced concrete buildings, *Earthquake Engineering & Structural Dynamics*, 45(5), 797-817.

Brown, MB, Forsythe, AB. (1974). Robust tests for the equality of variances. *Journal of the American Statistical Association*. 69: 364–367.

Kruskal WH, Wallis WA (1952). Use of Ranks in One-Criterion Variance Analysis. *Journal of the American Statistical Association*. 47 (260): 583–621.

Marsaglia, G, Tsang W, Wang, J (2003). Evaluating Kolmogorov's Distribution. *Journal of Statistical Software*; 8(18).

Ramirez CM, Miranda E (2012). Significance of residual drifts in building earthquake loss estimation. *Earthquake Engineering & Structural Dynamics*, 41, 1477–1493.

Romão X, Delgado R, Guedes J, Costa A (2014). Probabilistic performance analysis of existing buildings under earthquake loading. *Journal of Earthquake Engineering*; 18(8) 1241-1265.